

## Critical current density obtained from particle-size dependence of magnetization in $\text{YBa}_2\text{Cu}_3\text{O}_{7-\delta}$ powders

E. Shimizu and D. Ito

*Toshiba Research and Development Center, Toshiba Corporation, 4-1, Ukishima-cho, Kawasaki-ku, Kawasaki-shi Kanagawa 210, Japan*

(Received 2 November 1988)

The authors have measured the magnetization for a number of different sized  $\text{YBa}_2\text{Cu}_3\text{O}_{7-\delta}$  powders. The magnetization is in linear proportion to the particle size over the 1–20- $\mu\text{m}$  range and saturates at above 20  $\mu\text{m}$ . Critical current density in the  $\text{YBa}_2\text{Cu}_3\text{O}_{7-\delta}$  powder, obtained from the slope of the linear proportion part based on the Bean model, is  $2 \times 10^6 \text{ A/cm}^2$  at 4.2 K, 0.3 T, and  $7 \times 10^4 \text{ A/cm}^2$  at 77 K, 0.03 T. The magnetization saturation suggests that the current flow responsible for the magnetization is limited by grain boundaries in the  $\text{YBa}_2\text{Cu}_3\text{O}_{7-\delta}$  powder, whose particle diameter is larger than 20  $\mu\text{m}$ .

Since the discovery of the 90-K class critical temperature superconductor  $\text{YBa}_2\text{Cu}_3\text{O}_{7-\delta}$ ,<sup>1</sup> a number of groups have reported the critical current density,  $J_c$ , determined by the four-probe method for sintered bulk samples. These  $J_c$  values, at most approximately  $10^4 \text{ A/cm}^2$  at 77 K, 0 T,<sup>2-4</sup> are lower than the  $J_c$  value obtained for single crystals with magnetization method,<sup>5</sup> approximately  $10^7 \text{ A/cm}^2$  at 4.2 K, 0 T. In order to reveal the reason for the low  $J_c$  value in bulk sintered samples, the authors have studied the size dependence of magnetization for  $\text{YBa}_2\text{Cu}_3\text{O}_{7-\delta}$  powders. A similar experiment for  $\text{YBa}_2\text{Cu}_3\text{O}_{7-\delta}$  powders, made by a solid reaction method, was reported.<sup>6</sup> However, no systematic measurements on the size dependence for the  $\text{YBa}_2\text{Cu}_3\text{O}_{7-\delta}$  system magnetization were reported yet.

This paper reports the magnetic properties on some

$\text{YBa}_2\text{Cu}_3\text{O}_{7-\delta}$  powders calcined in air, with average particle diameters ranging from 3–53  $\mu\text{m}$ . These data provide information about the attainable maximum  $J_c$  for sintered bulk materials and the reason for the low  $J_c$ .

Raw material was made using a coprecipitated method. It was heated in air at a rate of  $50^\circ\text{C}$  per hour, up to  $950^\circ\text{C}$ , fired at  $950^\circ\text{C}$  for 10 h, and cooled at a rate of  $50^\circ\text{C}$  per hour down to room temperature. After milling the material into powders, samples were prepared by passing these powders through a 100-mesh sieve and then separating them into different size particles (average diameters ranging from 3–53  $\mu\text{m}$ ) by a Donaldson classifier. Table I shows the average diameters for 16 samples. The size distribution for each sample was determined with dry sieves and a coulter counter, which is based on the x-ray absorption of the particles during their sedimentation in NaCl liquid.

Figure 1 shows the temperature dependence of magnetization for sample 1. Flux-exclusion data were obtained

TABLE I. Properties for  $\text{YBa}_2\text{Cu}_3\text{O}_{7-\delta}$  powders.  $D^{25}$ ,  $D^{50}$ , and  $D^{75}$  indicate average diameters for cumulative weight distribution at 25%, 50%, and 75%, respectively.

Sample no.	$D^{25}$	Diameters $D^{50}$ ( $\mu\text{m}$ )	$D^{75}$	Packing density (%)
1	2.6	3.1	3.7	29
2	4.0	4.8	5.8	38
3	6.6	7.7	9.2	44
4	7.0	8.8	10.5	51
5	7.0	10.0	12.5	49
6	13.0	15.2	17.9	52
7	16.0	19.2	22.1	55
8	16.5	20.4	24.5	55
9	16.0	21.5	25.5	55
10	9.5	23.1	43.0	56
11	12.4	24.9	45.1	53
12	18.2	26.7	38.8	57
13	22.1	32.3	46.0	57
14	25.0	34.8	48.0	53
15	18.0	36.0	63.5	57
16	26.5	52.5	74.0	58

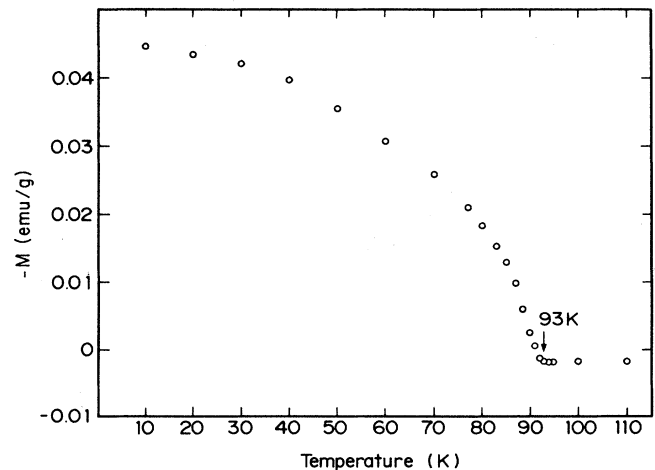


FIG. 1. Magnetization temperature dependence at 20 G for sample 1. These data are obtained from a flux exclusion process. Superconducting onset temperature is 93 K.

in a 20-G field with a SQUID magnetometer. This result indicates that the critical temperature,  $T_c$ , value for these samples is 93 K.

Most magnetization measurements were carried out with dc magnetization measurement systems, which have two coaxial search coils in a back up field coil. The back up coil can generate a magnetic field up to 2 T at 4.2 K and up to 1 T at 77 K. The samples are packed in the form of a hollow cylinder, whose densities are listed in Table I. Sample volumes were corrected with these values, in the magnetization calculation.

Typical magnetization loops at 4.2 K are shown in Fig. 2 obtained for samples 1, 6, 15, and 16. This figure shows that the magnetization decreases with decreasing powder size.

The magnetization loop width  $\Delta M$ , as defined in Fig. 2, can be explained based on the Bean model, as follows:

$$\Delta M = \frac{\mu_0 d J_c}{2}, \quad (1)$$

where  $\mu_0$  is permeability in a vacuum and  $d$  is the mean diameter,  $D^{50}$  for each powder particle. Average  $J_c$  values in individual particles can be derived from the slope of the  $\Delta M$  versus the powder diameter relationship.

Figure 3 shows the  $\Delta M$  dependence on powder size at 4.2 K for 0.3, 0.5, and 0.8 T. The magnetization at 4.2 K for every field measured is in linear proportion to particle size over the 1–20- $\mu\text{m}$  range and saturates at above 20

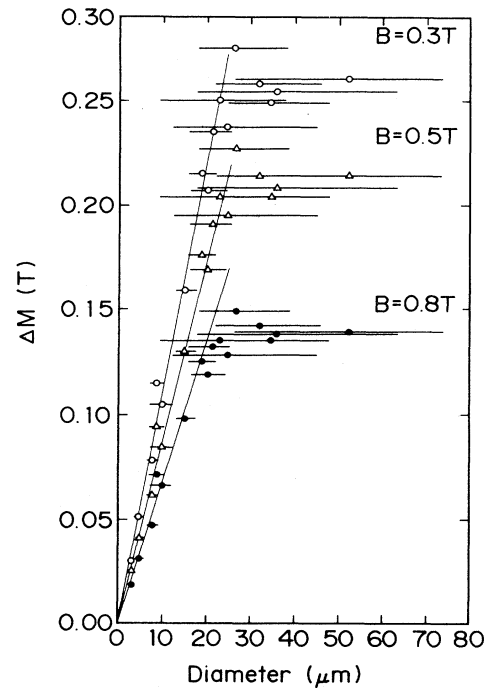


FIG. 3. Magnetization powder diameter dependence at 4.2 K. Horizontal bar cover diameter distribution from  $D^{25}$  to  $D^{75}$  and central points show  $D^{50}$ .

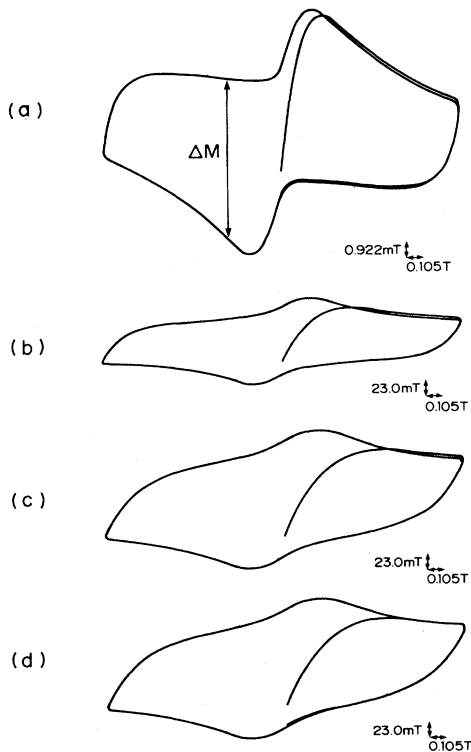


FIG. 2. Magnetization curves at 4.2 K. (a) Sample 1 ( $D^{50} = 3.1 \mu\text{m}$ ); (b) sample 6 ( $D^{50} = 15.2 \mu\text{m}$ ); (c) sample 15 ( $D^{50} = 36.0 \mu\text{m}$ ); (d) sample 16 ( $D^{50} = 52.2 \mu\text{m}$ ).

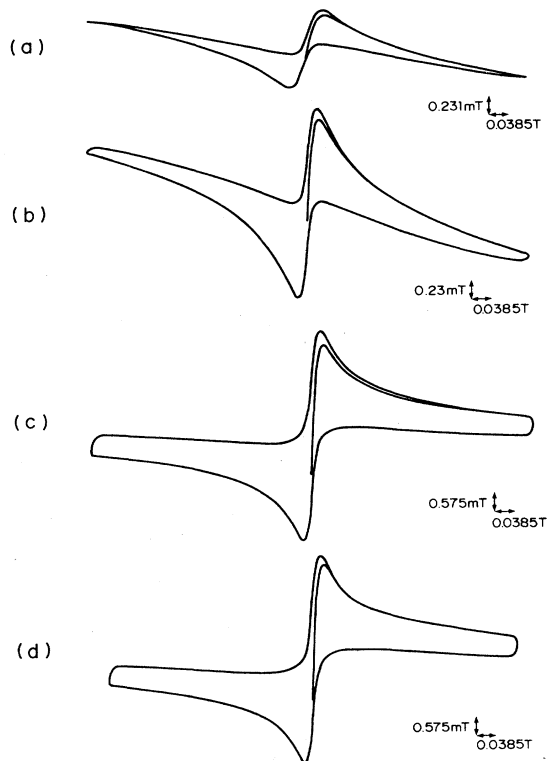


FIG. 4. Magnetization curves at 77 K. (a) Sample 1 ( $D^{50} = 3.1 \mu\text{m}$ ); (b) sample 2 ( $D^{50} = 4.8 \mu\text{m}$ ); (c) sample 9 ( $D^{50} = 21.5 \mu\text{m}$ ); (d) sample 15 ( $D^{50} = 36 \mu\text{m}$ ).

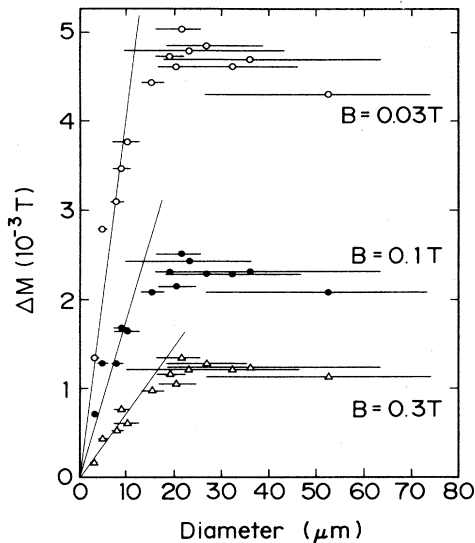


FIG. 5. Magnetization powder diameter dependence at 77 K. Horizontal bars cover diameter distribution, from  $D^{25}$  to  $D^{75}$ , and central points show  $D^{50}$ .

$\mu\text{m}$ . The  $J_c$  value, derived from Eq. (1), is approximately  $2 \times 10^6 \text{ A/cm}^2$  at 4.2 K, 0.3 T from the slope in the linear relationship.

Typical magnetization loops at 77 K are also shown in Fig. 4 for samples 1, 2, 9, and 15. These magnetizations are smaller than those in Fig. 2. Figure 5 shows the  $\Delta M$  dependence on powder size at 77 K for 0.03, 0.1, and 0.3 T. The magnetization at 77 K for every field measured is also in linear proportion to the powder size over the 1–20- $\mu\text{m}$  range and saturates above 20  $\mu\text{m}$ .  $J_c$  at 77 K is obtained as approximately  $7 \times 10^4 \text{ A/cm}^2$  at 0.03 T.

These  $J_c$  values are almost the same or somewhat larger, compared with that for the single crystal.<sup>5</sup>

The magnetization saturation indicates that major magnetization current cannot flow through boundaries on a 20- $\mu\text{m}$ -wide region. A similar result, that  $\Delta M$  depends little upon thickness of the sintered  $\text{YBa}_2\text{Cu}_3\text{O}_{7-\delta}$  plates, was reported,<sup>7</sup> whose thickness ranged from 180–1050  $\mu\text{m}$  at 77 K. On the other hand, a result<sup>8</sup> obtained for  $\text{DyBa}_2\text{Cu}_3\text{O}_{7-\delta}$  powders was different from the author's result, in that the magnetic moment, obtained from Campbell's method,<sup>9</sup> is independent from the particle size over the 3–12- $\mu\text{m}$  range at 4.2 K.

Figure 6 shows a typical transmission electron microscopy, TEM, micrograph for a particle in sample 1, whose average powder size is 3  $\mu\text{m}$ . It is shown that twin boundaries are arrayed and there are several bend contours through the particle. Therefore, this particle was made from a single crystal.



FIG. 6. Transmission electron microscopy (TEM) micrograph for a particle in sample 1. The arrow points to bend contour.

Not only the TEM observation result, but also estimated grain size in  $\text{YBa}_2\text{Cu}_3\text{O}_{7-\delta}$ ,<sup>10</sup> suggest that an individual particle, whose average powder sizes are smaller than 20  $\mu\text{m}$ , is made of a single crystal or its fragment. On the other hand, each particle whose powder size is larger than 20  $\mu\text{m}$  seems to be made of several grains. Therefore, the magnetization saturation can be explained with a model wherein current flow over the 20- $\mu\text{m}$  range is limited by grain boundaries.

In summary, magnetization at 4.2 and 77 K for the field measured is in linear proportion to powder size at over 1–20  $\mu\text{m}$  and saturates at above 20  $\mu\text{m}$ .  $J_c$  values, obtained from the slope in the linear relationship, are approximately  $2 \times 10^6 \text{ A/cm}^2$  at 4.2 K, 0.3 T, and approximately  $7 \times 10^4 \text{ A/cm}^2$  at 77 K, 0.03 T. The current flow over the 20- $\mu\text{m}$  range seems to be limited by the grain boundaries.

The authors wish to thank S. Nakamura and S. Takeno for their help in TEM observation and H. Kawagishi for assistance in experiments.

<sup>1</sup>M. K. Wu *et al.*, Phys. Rev. Lett. **58**, 908 (1987).

<sup>2</sup>Y. Yamada *et al.*, Jpn. J. Appl. Phys. **26**, L865 (1987).

<sup>3</sup>N. Sadakata (unpublished).

<sup>4</sup>S. Jin *et al.*, Appl. Phys. Lett. **52**, 2074 (1988).

<sup>5</sup>T. R. Dinger, T. K. Worthington, W. J. Gallagher, and R. J. Sandstorm, Phys. Rev. Lett. **58**, 2687 (1987).

<sup>6</sup>A. D. Hibbs, F. J. Eberhardt, A. M. Campbell, and S. Male,

Cryogenics **28**, 678 (1988).

<sup>7</sup>K. Funaki *et al.*, Jpn. J. Appl. Phys. **26**, L1445 (1987).

<sup>8</sup>M. Daeumling, J. Seuntjens, and D. C. Larbalestier, Appl. Phys. Lett. **52**, 590 (1988).

<sup>9</sup>A. M. Campbell, J. Phys. C **2**, 1492 (1969).

<sup>10</sup>R. L. Peterson and J. W. Ekin, Phys. Rev. B **37**, 9848 (1988).



FIG. 6. Transmission electron microscopy (TEM) micrograph for a particle in sample 1. The arrow points to bend contour.